

Modeling and Fault Characteristic Analysis of Grid-forming Electrochemical Energy Storage

Yuanhang Xu
School of Electrical
Engineering
Beijing Jiaotong University
Beijing, China
23121499@bjtu.edu.cn

Jinghan He
School of Electrical
Engineering
Beijing Jiaotong University
Beijing, China
jhhe@bjtu.edu.cn

Meng Li
School of Electrical
Engineering
Beijing Jiaotong University
Beijing, China
lmeng@bjtu.edu.cn

Xiaotong Du
School of Electrical
Engineering
Beijing Jiaotong University
Beijing, China
22110453@bjtu.edu.cn

Xiang Chen
School of Electrical
Engineering
Beijing Jiaotong University
Beijing, China
22121435@bjtu.edu.cn

Guohong WU
Dept. of Electrical & Electronics
Eng.
Tohoku Gakuin University
Miyagi, Japan
wugh@mail.tohoku-gakuin.ac.jp

Abstract—With the extensive application of energy storage technology, electrochemical energy storage has become a hot solution for addressing the challenges of integrating new energy sources into the grid. However, the switching between charging and discharging modes and the differences in control strategies can all impact the fault characteristics of energy storage systems. Therefore, it is necessary to conduct a comprehensive and in-depth analysis of their fault characteristics. This paper establishes a grid-forming energy storage power station system model based on the system topology and control strategies of energy storage power stations. It simulates the differences in characteristics under normal operation and fault ride-through scenarios in both charging and discharging modes, and analyzes the reasons for these differences. Finally, a grid-forming energy storage power station simulation model is built on PSCAD, providing a reference for subsequent research on the protection and control strategies of grid-forming energy storage grid-connected systems.

Keywords—Electrochemical energy storage, grid-forming control, fault characteristic analysis, fault ride-through.

I. INTRODUCTION

Currently, environmental issues are intensifying, and the world is focusing on two key topics: "carbon peak" and "carbon neutrality". In the power industry, generating electricity from renewable energy sources such as wind and solar energy is one of the effective ways to address this challenge. However, renewable energy sources like wind power and photovoltaic have significant differences from traditional energy sources in terms of power generation principles and control methods. As their proportion in the power system increases, the stability, operation, and planning of the system face significant changes. The main challenge lies in dealing with the intermittency of renewable energy and the uncertainty brought by the electrification of power [1]. In the context of a smart grid, energy

storage technology is crucial for the integration and utilization of large-scale new energy. Energy storage technology is the core of achieving flexible conversion and comprehensive utilization of electrical energy with other forms of energy, solving the problem of mismatch between energy production and consumption in terms of time and space, and enhancing the mobility and shareability of energy [2-4], among which electrochemical energy storage technology is relatively mature. The use of power electronic devices in energy storage systems and the four-quadrant operation characteristics of energy storage increase the complexity of system faults. Among them, the ways of inverter-type energy storage access are divided into grid-following and grid-forming, compared with grid-following control (GFLC), grid-forming control (GFMC) technology can make better use of the flexibility and controllability of voltage source converters (VSC). This technology shows excellent adaptability and stability in weak power grids, capable of quickly autonomously constructing system voltage, and supplementing the system's missing inherent inertia and damping characteristics, providing stable voltage and frequency support for the power grid [5]. Therefore, it is very necessary to establish a grid-forming energy storage power station model suitable for fault analysis and to study its fault characteristics under different conditions.

Currently, scholars have conducted extensive research on the construction of simulation models and the study of fault characteristics of electrochemical energy storage power stations. Reference [6] discusses the electromagnetic transient behavior of lithium-ion batteries under AC grid faults and analyzes the impact of the battery's state of charge (SOC) and converter control strategy on fault current characteristics. References [7-8] have constructed multi-timescale energy storage models to explore the electromechanical transient and medium to long-term dynamic characteristics of battery energy storage systems. Reference [9] has developed an energy storage model suitable for electromechanical transient analysis using virtual

This work is supported by National Natural Science Foundation of China (Grant No.U23B6007,Fundamental Theory and Methods for Form Evolution and High Efficient Safe Operation of New Power Distribution Systems).

synchronous machine technology. References [10-11] have built an electromechanical transient model of an energy storage system considering the charging and discharging power of batteries in the PSASP simulation environment, and the models uniformly adopt frequency-active power control and voltage-reactive power control strategies. Reference [12] discusses the dynamic behavior of energy storage power stations under grid faults and points out that the differences in characteristics exhibited by energy storage power stations in charging and discharging states are a key factor that needs to be considered in relay protection. Reference [13] proposes an electromagnetic transient modeling method for lithium battery energy storage systems and analyzes the differences in fault characteristics of energy storage power stations under different charging and discharging modes. Existing literature mostly focuses on modeling energy storage power stations in grid-following mode, and models with grid-forming control are mostly concentrated on new energy sources such as photovoltaics. Moreover, there is more analysis on fault characteristics under discharging states. Therefore, existing research is insufficient to reflect the fault characteristics of grid-forming energy storage systems. To analyze the fault characteristics of grid-forming energy storage systems, this paper takes lithium-ion battery energy storage as the research subject and establishes an electromagnetic transient model of the energy storage system for both normal operation and fault operation conditions. Furthermore, it compares and analyzes the operational differences of energy storage in charging and discharging modes.

II. ENERGY STORAGE POWER STATION TOPOLOGY

A. Energy Storage Power Station

The grid-connected electrochemical energy storage system adopts a dual-stage topology as shown in Fig.1, which has a wider operating voltage range compared to a single-stage type. The grid-connected system consists of lithium-ion energy storage, a bidirectional DC/DC converter(BDC), an energy storage power converter system(PCS), and an LC filter. The lithium battery is boosted by the BDC, then connected to the AC grid after being inverted by the PCS and filtered by the filter. The BDC is used to maintain the stability of the DC-side voltage and to meet the power transmission requirements in both charging and discharging modes. The PCS employs virtual synchronous control to independently control the AC-side voltage, frequency, active power, and reactive power, possessing strong frequency and voltage support capabilities. In the figure, E_{bat} and R_{bat} represent the internal electromotive force and internal resistance of the lithium battery energy storage, C_1 and C_2 are the capacitors on the low-voltage side and high-voltage side of the DC/DC converter, respectively, U_{dc} is the DC bus voltage, and L_N and C_N are the inductor and capacitor of the LC filter.

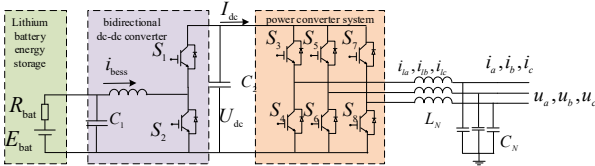


Fig. 1. Energy Storage Power Station Grid-connection System

B. Battery Model

In previous literature, various equivalent circuit models have been proposed. These include the RC model, Thevenin equivalent circuit model, PNGV model, Peuker model, and Shepherd model, among others. Among them, the Shepherd model has a relatively simple structure and is easy to implement and simulate on a computer. By adjusting the parameters in the model, it is possible to simulate different types of batteries and different operating conditions, and it can describe the dynamic response of batteries during the charging and discharging process, including transient and steady-state behavior.

The equivalent circuit model of the battery is shown in reference[14] which is represented as a controlled source in series with a resistor. The expression for the internal electromotive force is given by:

$$E_{bat} = E_0 - K \frac{Q}{Q - it} + A \cdot e^{-B \cdot it} \quad (1)$$

In the formula, E_{bat} represents the internal electromotive force, E_0 is the constant voltage of the battery; K is the polarization voltage; Q is the battery capacity; A is the amplitude of the exponential region; B is the inverse of the time constant in the exponential region; it is the electrical charge that the battery has absorbed/released. The parameters of the model are all calculated from the discharge characteristic curve of the battery, and the specific discharge characteristic curve can be found in reference [14].

The battery voltage equation can be modified as follows to replace it with the ratio of the remaining capacity to the total capacity, SOC, to represent:

$$E_{bat} = E_0 - K \frac{1}{SOC} + A \cdot e^{-B \cdot Q(1-SOC)} \quad (2)$$

III. GRID-CONNECTION SYSTEM CONTROL STRATEGY

A. BDC Control Strategy

The DC/DC converter is connected to the battery energy storage on one side and the DC side of the PCS on the other, and is used to maintain a constant DC bus voltage. The specific control strategy is shown in Fig.2. The control method adopts a dual-loop control, the specific control method is as follows: by setting a reference value for the outer loop DC voltage, a reference value for the inner loop current is given based on the difference, and the difference between the current reference value and the actual value is passed through a proportional-integral controller to obtain the duty cycle of the thyristors S1 and S2, ultimately obtaining the triggering signal.

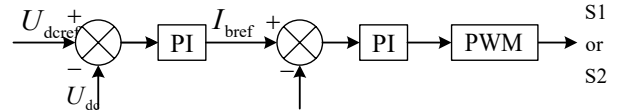


Fig. 2. Control Strategy for Constant DC Bus Voltage

B. PCS Control Strategy

As shown in Fig.1 and Fig.3, the four-quadrant operation function of the energy storage system is realized by controlling

the conduction and interruption of the switching tubes. The PCS adopts grid-forming control, with the specific control method being virtual synchronous machine control.

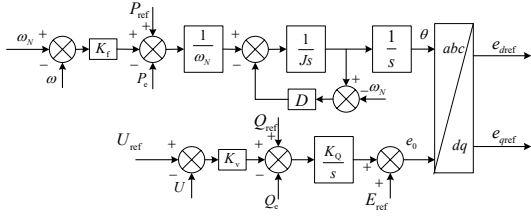


Fig. 3. Virtual Synchronous Machine Control

The control method during the normal operation mode of the energy storage system is as follows: the outer loop consists of a virtual synchronous control loop, which includes two parts: active power-frequency control loop and reactive power-voltage control loop. In Fig.3., P_{ref} and P_e represent the reference and actual values of active power, respectively; Q_{ref} and Q_e represent the reference and actual values of reactive power, respectively. J , D , K_f , K_v , K_Q , ω , and ω_N represent virtual inertia, virtual damping, active power frequency control coefficient, reactive power voltage control coefficient, reactive power voltage integral coefficient, virtual internal electromotive force angular frequency, and rated angular frequency, respectively. U_{ref} is the base voltage value, while E_{ref} is the static working point electromotive force. During normal operation, U_{ref} equals U_N . The active power-frequency control loop simulates the motion equation of the generator rotor [15], providing damping and inertia support to the power grid, and outputs the virtual internal electromotive force phase angle θ . The reactive power-voltage control loop simulates the excitation of the synchronous machine to simulate the reactive power-voltage regulation characteristics, outputting the virtual internal electromotive force amplitude e_0 . The basic control equations for both are as follows:

$$\begin{cases} J \frac{d^2 \theta}{dt^2} = \frac{P_{ref} - P_e}{\omega_0} - D(\omega - \omega_0) \\ e_0 = \frac{K_Q}{S} (K_v (U_{ref} - U) + Q_{ref} - Q) + E_{ref} \end{cases} \quad (3)$$

As shown in Fig.4, the intermediate link is a virtual impedance loop. By simulating the internal impedance characteristics of the synchronous generator, it effectively enhances the operational stability of virtual synchronous control.

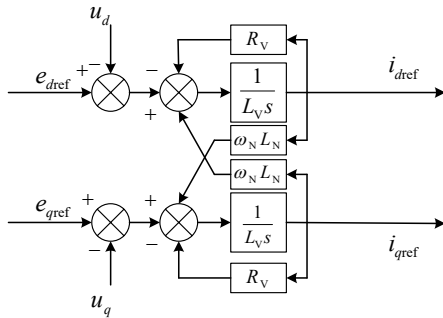


Fig. 4. Virtual Impedance Link

The basic control equation is as follows:

$$\begin{cases} e_{dref} - u_d = L_v \frac{di_{dref}}{dt} + R_v i_{dref} - \omega_N L_N i_{qref} \\ e_{qref} - u_q = L_v \frac{di_{qref}}{dt} + R_v i_{qref} + \omega_N L_N i_{dref} \end{cases} \quad (4)$$

In the formula, in the virtual synchronous control link, the virtual impedance control link includes L_N , L_v and R_v as the actual inductance, virtual resistance, and inductance values, respectively. e_{dqref} and u_{dq} are the d-axis and q-axis component values of the virtual internal electromotive force and the grid connection point voltage, respectively.

The final link is the inner current loop, which is similar to the current control link in traditional grid-following control. The control still uses PI control to achieve current tracking, and the basic control equation is as follows:

$$\begin{cases} V_d = K_p (i_{dref} - i_{ld}) + K_i \int (i_{dref} - i_{ld}) dt - \omega_N L_e i_{qref} + u_d \\ V_q = K_p (i_{qref} - i_{lq}) + K_i \int (i_{qref} - i_{lq}) dt + \omega_N L_e i_{dref} + u_q \end{cases} \quad (5)$$

In the formula, V_{dq} represents the reference value of the converter's dq-axis voltage, i_{dqref} and i_{ldq} represent the reference and actual values of the converter's dq-axis current, respectively, and K_p and K_i are the proportional and integral coefficients of the PI control loop.

C. Fault Ride-Through Control

When an external short circuit fault occurs, the topology of the external network changes accordingly, which may cause a certain fluctuation in the grid connection point voltage. Therefore, it is necessary to change the control strategy under the normal operation model to prevent excessive fault current from damaging the equipment, and to continue operating without disconnecting from the grid after the fault occurs. Thus, a fault ride-through control strategy is introduced during the fault period. The conventional fault ride-through control strategy is similar to the traditional grid-following fault ride-through control strategy, which abandons the outer loop control after the fault and directly controls the current loop. However, in order to maintain the high inertia characteristics of the virtual synchronous machine, this paper uses a fault ride-through control strategy that does not change the original control characteristics. Only the voltage reference value of the reactive power loop is changed to track the actual value of the grid connection point voltage. The active power and reactive power are given by the following formulas:

$$Q_{ref} = \begin{cases} 0, U > 0.8U_N \\ 1.5(0.8 - \frac{U}{U_N})I_N U, U \in [0, 0.8U_N] \end{cases} \quad (6)$$

In the formula, U_N represents the rated voltage, and I_N represents the rated current.

Based on the reactive power reference value, the formula for the active power reference value can be derived as follows:

$$P_{\text{ref}} = \begin{cases} P_{\text{ref}0}, & U > 0.8U_N \\ |U|I_{\text{P-ref}} = |U|\sqrt{I_N^2 - \left(1.5\left(0.8 - \frac{U}{U_N}\right)I_N\right)^2}, & U \in [0, 0.8U_N] \end{cases}, \quad (7)$$

In the formula, $P_{\text{ref}0}$ represents the initial power reference value, and $I_{\text{P-ref}}$ represents the active current value.

When an unbalanced fault occurs during power grid operation, it causes the generation of negative sequence currents, increasing the degree of grid imbalance. To ensure the safety and stability of the power system, a negative sequence control strategy is introduced to reduce the impact of negative sequence currents. This control strategy is mainly implemented through the inner current loop, where the negative sequence current is directly given a reference value of 0 through the inner loop, thereby effectively suppressing the negative sequence current. The positive sequence components continue to maintain their original control strategy.

IV. MODEL VERIFICATION AND FAULT ANALYSIS

To verify the effectiveness of the constructed energy storage power station model and its control strategy, and to further analyze the complex fault characteristics of the energy storage power station, an energy storage grid-connected system is built on the PSCAD/EMTDC simulation platform. A configuration of 20 battery energy storage systems with a capacity of 0.5MWh each is used, connected through a 380V/10kV transformer and then through a 2km transmission line for grid connection. Model validity and fault analysis are conducted under different scenarios.

A. Normal Operation Mode

First, set the energy storage to discharge mode with an initial capacity of 50%. The discharge power is set to 0.015MW. At 1.9 seconds, switch the discharge mode to charge mode. The power transition and phase change curves are shown in Fig.5. and Fig.6, respectively.

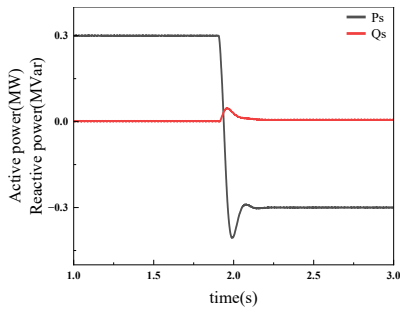


Fig. 5. Power Change Curve for Normal Mode Charge-Discharge Transition

It can be seen that after the mode switch command is initiated, the power can quickly track the specified value and stabilize around -0.015MW. As shown in Fig.6, the phase difference between voltage and current changes from 0° to approximately 180° . The experimental results indicate that the model can quickly respond to the transition between charge and discharge modes.

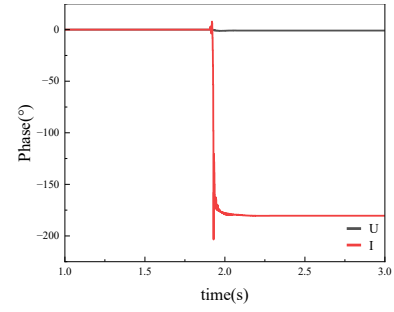
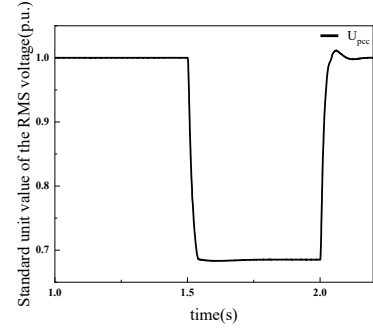


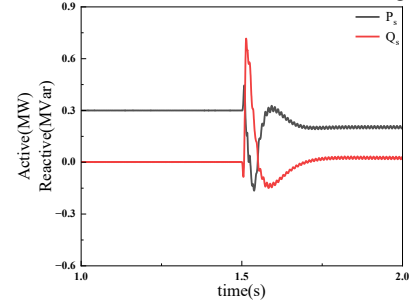
Fig. 6. Voltage and Current Phase Relationship During Normal Mode Charge-Discharge Transition

B. Fault Ride-Through Capability

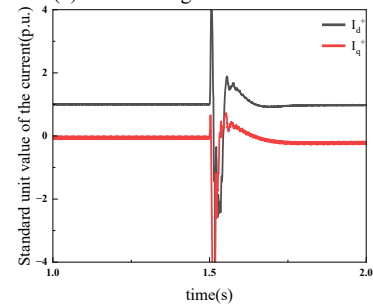
For the energy storage system in discharge mode, a single-phase grounding fault is set at the end of the outgoing line, and the fault is initiated at 1.5 seconds. As shown in Fig.7, the figures depict the effective value of the grid connection point voltage, fault power, dq-axis positive and negative sequence currents, and the AC-side current waveform.



(a) Effective Value of Grid Connection Point Voltage



(b) Power Change Waveform



(c) Positive Sequence dq-Axis Current

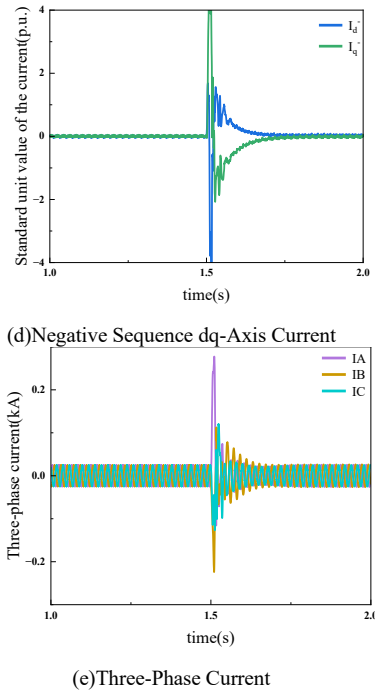
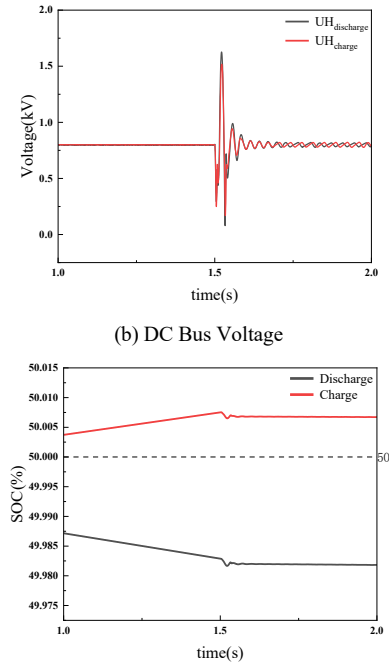
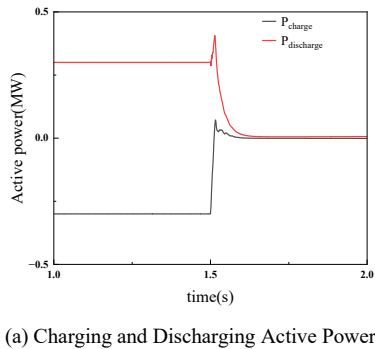


Fig. 7. Unsymmetrical Fault Simulation Results

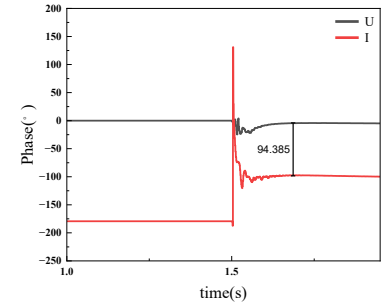
As shown in Fig.7(a), after the fault occurs, the grid connection point voltage drops to around 0.69 p.u. As shown in Fig.7(b) and 7(c), to support the voltage and prevent overcurrent, the fault control strategy changes the reference value of the power loop, and the positive sequence current changes in response to the reference value of the power loop, with a similar trend. Due to the implementation of a negative sequence current suppression strategy, the negative sequence current component is suppressed to zero, as shown in Fig.7(d). Due to changes in the working state and the PCS control strategy, the reference values of the d and q-axis currents change abruptly, causing the output current amplitude and phase to change abruptly. The amplitude of the fault steady-state current is about 1.05 times the rated current, as shown in Fig.7(e).

C. Differences in Fault Characteristics between Charging and Discharging Scenarios

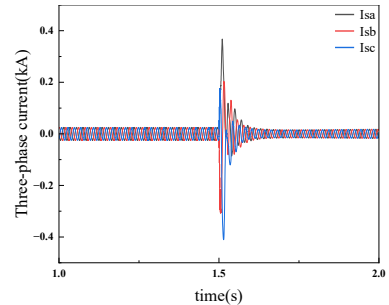
To analyze the impact of charging and discharging modes on fault characteristics, the energy storage power station is set to operate in charging and discharging modes at the start of the simulation, with a three-phase non-metallic short circuit fault set at the end of the outgoing line, and the fault is initiated at 1.5 seconds. The simulation results are shown in Fig.8.

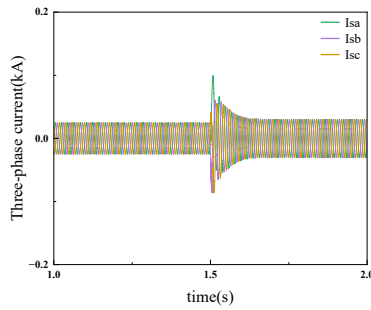


(d) Phase Relationship between Voltage and Current in Charging Mode



(e) Phase Relationship between Voltage and Current in Discharging Mode





(g) Three-Phase Current during Shallow Voltage Dip in Discharging Mode

Fig. 8. Charging/Discharging Fault Simulation Results

As shown in Fig.8(a), it can be seen that under normal charging and discharging modes, when the voltage drops, the power reference value changes, and it is lower than the reference value under normal operation mode. However, due to the constant voltage control of the BDC, the power absorbed/released by the energy storage is consistent with the power transmitted by the PCS, as shown in Fig.8(b), the DC bus voltage can still be maintained at around 0.8kV after the fault. But the rate of change of SOC is slowed down, as shown in Fig.8(c). As shown in Fig.8(d) and 8(e), The phase difference between voltage and current exists after the fault due to the different directions of active power transmission in charging/discharging modes. Therefore, when conducting related research in relay protection, it is necessary to consider the impact of the phase difference caused by charging/discharging modes on the protection strategy.

The magnitude of the fault current is related to the degree of voltage drop at the grid connection point, and since the power reference value is proportional to the grid connection point voltage. When the degree of voltage drop at the grid connection point is large, the fault current after the fault is less than the rated current, as shown in Fig.8(f), which may cause the protection to fail to act. When the grounding resistance is changed to 1Ω and the degree of voltage drop at the grid connection point is lower, the fault current is greater than the rated current, about 1.2 times the rated current, as shown in Fig.8(g), and the protection setting value can be set according to the current magnitude.

V. CONCLUSION

This paper, based on the structure and control strategy of the electrochemical energy storage power station, has established a simulation model of the energy storage power station. It focuses on analyzing the fault characteristics of the energy storage power station under charging/discharging scenarios and considers the impact of the degree of voltage dip. The main conclusions are as follows:

1) The proposed model can respond to power command changes in a timely manner, quickly switch between charging and discharging states, and achieve stable regulation of transmitted power; it has fault ride-through capabilities and can reflect the fault characteristics of the energy storage power station under charging/discharging scenarios.

2) Under charging/discharging scenarios, when a grid-side fault causes a deep voltage dip at the grid connection point of the energy storage power station, the steady-state fault current is less than the rated working current; when the dip is shallow, the fault current is generally greater than the rated working current; the particularity of this fault characteristic may have a certain impact on existing current protection schemes or settings.

3) In charging/discharging scenarios, after a fault occurs on the grid side, the energy storage power station can still achieve stable DC bus voltage and balance the power transmission on both sides of the PCS through constant voltage control of the BDC.

REFERENCES

- [1] KANG C, YAO L. Key scientific issues and theoretical research framework for power systems with high proportion of renewable energy [J]. *Automation of Electric Power Systems*, 2017, 41(9): 1-11.
- [2] Zhou L, Huang Y, Guo K, et al. A Review of Energy Storage Technology in Microgrids. *Electric Power Systems Research*, 2011, 39(7): 147-152.
- [3] Yuan, X., Cheng, S., Wen, J. Prospects of energy storage technology in addressing the challenges of large-scale wind power integration. *Automation of Electric Power Systems*, 2013, 37(1): 14-18.
- [4] Luo, X., Wang, J., Ma, Z. A review of energy storage technologies and their application prospects in smart grids. *Smart Grid*, 2014, 2(1): 7-12.
- [5] Wang, L., Hu, P., Yu, Y., et al. Transient stability analysis of grid-forming converters under asymmetrical faults based on hybrid synchronous control. *Automation of Electric Power Systems*, 1-15 [2024-09-10].
- [6] SALEH SA, OZKOP E, VALDES M E, et al. On the factors affecting battery unit contributions to fault currents in grid-connected battery storage systems[J]. *IEEE Transactions on Industry Applications*, 2022, 58(3): 3019-3028.
- [7] Lu, Q., Hu, W., Zheng, L., et al. Multi-timescale modeling and analysis application of battery energy storage systems. *Proceedings of the CSEE*, 2013, 33(16): 86-93, 14.
- [8] Ye, X., Liu, T., Wu, G., et al. Research on multi-timescale simulation modeling of battery energy storage systems and analysis of large-scale grid-connected characteristics. *Proceedings of the CSEE*, 2015, 35(11): 2635-2644.
- [9] He, P., Li, Z., Li, C., et al. Modeling of electromechanical transient characteristics of energy storage based on virtual synchronous machine technology. *Electric Power System Protection and Control*, 2022, 50(7): 11-22.
- [10] Li, J., Niu, M., Zhang, B., et al. Electromechanical Transient Simulation Model of Battery Energy Storage System. *Transactions of China Electrotechnical Society*, 2018, 33(8): 1911-1918.
- [11] Li, Y., Jing, P., Wang, L., et al. Research on the Mathematical Model of Universal Energy Storage System and Its PSASP Modeling. *Power System Technology*, 2012, 36(1): 51-57.
- [12] BERGER M, KOCAR I, FARANTATOS E, et al. Modeling of Li-ion battery energy storage systems (BESSs) for grid fault analysis[J]. *Electric Power Systems Research*, 2021, 196: 107160.
- [13] Zhang, J., Liu, P., Xie, X., et al. Electromagnetic Transient Modeling Method of Lithium-ion Battery Energy Storage for Fault Characteristic Analysis. *Automation of Electric Power Systems*, 2023, 47(7): 166-173.
- [14] Qi, L., Wang, X., Zhu, Y., et al. Modeling of Energy Storage Battery and PSCAD Simulation. *Electrical Applications*, 2014, 33(11): 85-89.
- [15] Jia L, Miura Y, Ise T. Comparison of Dynamic Characteristics Between Virtual Synchronous Generator and Droop Control in Inverter-Based Distributed Generators[J]. *IEEE Transactions on Power Electronics*, 2015, 31(5): 3600-3611.